Research in Astronomy and Astrophysics, 25:055018 (11pp), 2025 May
https://doi.org/10.1088/1674-4527/add111
CSTR: 32081.14.RAA.add111

Dependence of 4000 Å Break Strength on Narrow Emission Line Properties in Local Type-2 AGN

Xue-Guang Zhang
Guangxi Key Laboratory for Relativistic Astrophysics, School of Physical Science and Technology, GuangXi University, Nanning 530004, China; xgzhang@gxu.edu.cn
Received 2025 February 22; revised 2025 April 6; accepted 2025 April 25; published 2025 May 21

Abstract

In this manuscript, we report evidence to support the dependence of D*n*4000 (4000 Å break strength to trace stellar ages) on central active galactic nuclei (AGN) activity traced by narrow emission line properties in local Type-2 AGN in SDSS DR16. Based on the measured D*n*4000 and flux ratios of [O III] to narrow Hβ (O3HB) and [N II] to narrow Hα (N2HA) and narrow Hα line luminosity $L_{\rm H\alpha}$, linear dependence of the D*n*4000 on the O3HB, N2HA and $L_{\rm H\alpha}$ in the local Type-2 AGN can provide clues to support the dependence of D*n*4000 on properties with narrow emission lines. Linear correlations between the D*n*4000 and the O3HB and N2HA can be found in the local Type-2 AGN, with Spearman rank correlations of about −0.39 and 0.53. Meanwhile, stronger dependence of the D*n*4000 on the $L_{\rm H\alpha}$ can be confirmed in Type-2 AGN, with a Spearman rank correlation coefficient of about −0.7. Moreover, combining the $L_{\rm H\alpha}$ and the N2HA, a more robust and stronger linear correlation can be confirmed between the D*n*4000 and the new parameter LR = $0.2\log(L_{\rm H\alpha}) - 0.5\log({\rm N2HA})$, with a Spearman rank correlation coefficient of about −0.76 and with smaller rms scatters. After considering necessary effects, the dependence of D*n*4000 on LR is stable and robust enough for the local Type-2 AGN, indicating that the LR on the narrow emission lines can be treated as a better indicator to statistically trace stellar ages of samples of more luminous AGN with weaker host galaxy absorption features.

Key words: galaxies: active – galaxies: nuclei – (galaxies:) quasars: emission lines – galaxies: Seyfert

1. Introduction

Tight connections between active galactic nuclei (AGN) and host galaxies can be expected due to AGN feedback through galactic-scale outflows playing key roles in galaxy evolutions as discussed in McNamara & Nulsen (2007), Fabian (2012), Kormendy & Ho (2013), Heckman & Best (2014), King & Pounds (2015), Tombesi et al. (2015), Muller-Sanchez et al. (2018). Either negative or positive AGN feedback on star formations in AGN host galaxies have been reported and studied in both observational and theoretical results, such as clear evidence on negative AGN feedback in Feruglio et al. (2010), Page et al. (2012), Wylezalek & Zakamska (2016), Comerford et al. (2020), Zhang (2024a) and on positive AGN feedback in Zubovas et al. (2013), Zinn et al. (2013), Shin et al. (2019). Due to the contrary conclusions on effects of AGN feedback, it is interesting to provide further clues on the effects of AGN feedback through different methods.

Besides direct measurements of star formations, AGN feedback should have apparent and strong effects on stellar ages in AGN host galaxies. Different methods have been proposed to determine the mean stellar ages of galaxies. Cid Fernandes et al. (2005) have shown the measurements of light-weighted mean stellar ages by the STARLIGHT code based on the SSP (simple stellar populations) methods (Bruzual & Charlot 1993). Cappellari (2017) have shown that the penalized pixel-fitting method can lead to reliable and smoother star formation histories after considering the regularization method, then leads to estimated mass-weighted stellar ages. Kauffmann et al. (2003b) have estimated mean stellar ages by the parameters of D*n*4000 (4000 Å break strength) being applied to trace star-forming histories, similar discussions on D*n*4000 as an indicator to trace stellar ages can be found in Zahid et al. (2015). More recently, Greene et al. (2020) have shown the loose dependence of D*n*4000 on [O III] line luminosity, indicating narrow line luminosity could be roughly applied to trace stellar age properties.

Therefore, there are reliable methods to estimate stellar ages in AGN host galaxies. Certainly, in order to clearly estimate stellar ages, host galaxy features should be apparently significant in spectra, indicating Type-2 AGN (narrow emission line AGN) rather than Type-1 AGN (broad line AGN) are the better candidates to study effects of AGN activity on stellar ages. Moreover, based on the commonly accepted unified model (Netzer 2015; Suh et al. 2019) of AGN, emissions from central accretion disks, and from central broad emission line regions, are totally obscured by central dust torus in Type-2 AGN, indicating that both spectroscopic continuum emissions and absorption features

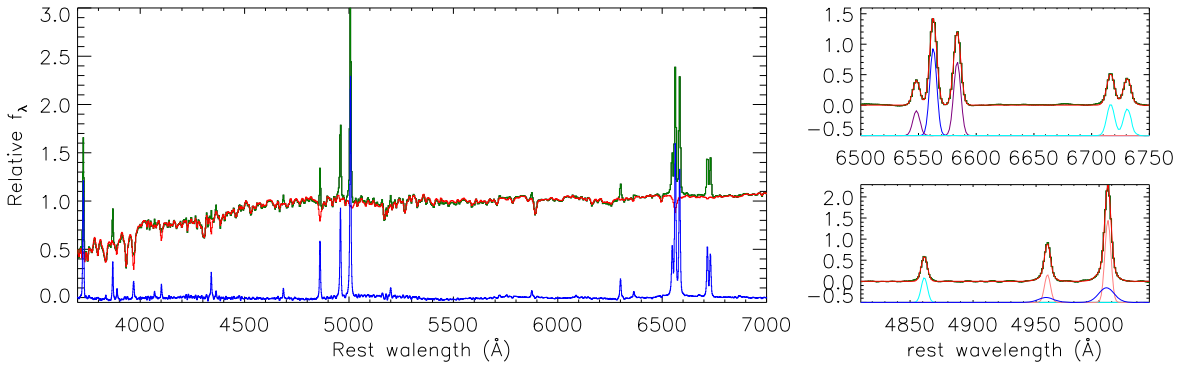

Figure 1. The left panel shows the SSP method determined best-fitting results (solid red line) to the host galaxy features in the inverse variance weighted mean spectrum (solid dark green line) of the Type-2 AGN, and the corresponding line spectrum (solid blue line) after subtractions of the host galaxy contributions. The right panels show the best-fitting results (solid red line) to the emissions lines (solid dark green line) around Hα (top right panel) and around Hβ (bottom right panel) in the mean spectra of Type-2 AGN, after subtractions of the host galaxy contributions. In the top right panel, solid lines in blue, in purple and in cyan show the determined narrow Hα, [N II] and [S II] doublets, respectively. In the bottom right panel, solid lines in blue, in pink and in cyan show the determined extended and core components of [O III] doublet, and narrow Hβ, respectively.

of Type-2 AGN can be clearly applied to measure the mean stellar ages with few contaminations.

Besides the host galaxy features in Type-2 AGN to determine stellar ages traced by the Dn4000 parameter mainly considered in this manuscript, the AGN activity of Type-2 AGN can be well traced by narrow emission line properties in the well-known BPT diagrams (Baldwin et al. 1981; Kewley et al. 2001; Kauffmann et al. 2003a; Kewley et al. 2006, 2019; Zhang et al. 2020). Therefore, there are sufficient conditions to do the research on the potential dependence of stellar ages on central AGN activity in a large sample of Type-2 AGN which can provide clear clues on effects of AGN feedback. This manuscript is organized as follows. Section 2 presents the data samples of Type-2 AGN, and the simple procedure to measure the Dn4000 parameter. Section 3 presents our main results and discussions. Section 4 gives our final summary and conclusions. And in this manuscript, we have adopted the cosmological parameters of $H_0 = 70\,\mathrm{km}\cdot\mathrm{s}^{-1}\,\mathrm{Mpc}^{-1}$, $\Omega_\Lambda = 0.7$ and $\Omega_\mathrm{m} = 0.3$.

2. Data Samples of Type-2 AGN

All the 87,828 low redshift narrow emission line galaxies are first collected from the main galaxies in the SDSS DR16 (Sloan Digital Sky Survey, Data Release 16, Ahumada et al. 2020) as the parent sample, with redshift smaller than 0.35 and with median spectral signal-to-noise ratio (S/N) larger than 10 and with SDSS-provided reliable narrow emission lines of Hβ, [O III], Hα and [N II] and with reliable SDSS pipeline-measured stellar velocity dispersions and with Balmer decrement (flux ratio of narrow Hα to narrow Hβ) smaller than 6. Meanwhile, we should note that the SDSS pipeline-provided emission line parameters have been collected from the database of "GalSpecLine" reported by MPA-JHU as described in Brinchmann et al. (2004), Tremonti et al. (2004), Kauffmann et al. (2003b), and the Dn4000are collected from the public SDSS database of "GalSpecIndx." Moreover, besides the SDSS pipeline provided values, the parameters of emission lines and Dn4000 have also been re-measured as follows.

Narrow emission lines have been re-measured in the collected narrow emission line objects, after subtractions of host galaxy contributions, in order to confirm the reliability of the narrow emission line parameters. Similar to what we have recently done in Zhang (2021a, 2021b, 2021c, 2022a, 2022b, 2023, 2024a), two main steps are applied. The first step is to determine the host galaxy contributions by the SSP method, as discussed in detail in Bruzual & Charlot (1993), Kauffmann et al. (2003a), Cid Fernandes et al. (2005), Cappellari (2017). The second step is to measure the emission lines by multiple Gaussian functions in the line spectrum after subtractions of host galaxy contributions. Here, we do not show further detailed discussions on the SSP method nor detailed discussions on measurements of emission lines any more, but Figure 1 shows an example on the SSP method determined host galaxy contributions in the inverse variance weighted mean spectrum of the collected Type-2 AGN, and the best fitting results to the emission lines, through the Levenberg–Marquardt least-squares minimization technique. Here, we do not show further discussions on the measured line parameters, but there are quite consistent line parameters between our measured values and the reported values in "GalSpecLine" for the narrow emission line galaxies, the correlations between SDSS-provided line intensities and our measured line intensities having Spearman Rank correlation coefficients larger than 0.93, to support the reliability of our measured emission line parameters.

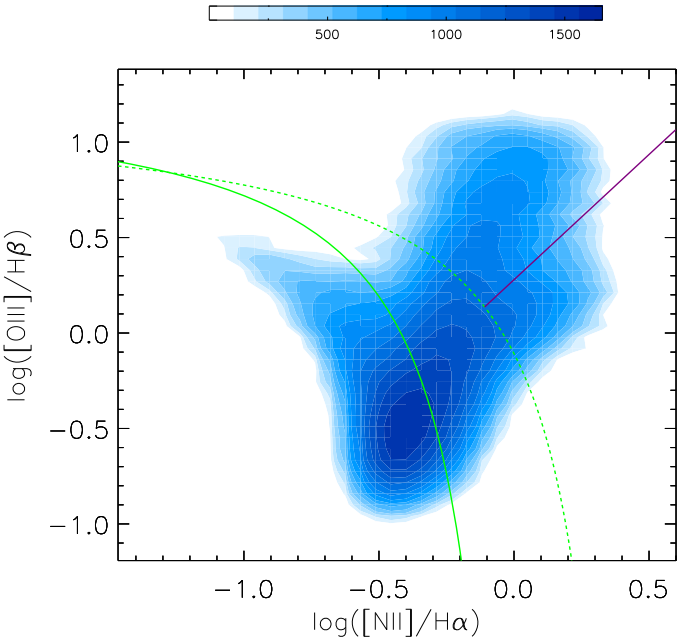

Figure 2. The BPT diagram of O3HB vs. N2HA for all the 87828 narrow emission line main galaxies in SDSS DR16, with all the collected 14031 Type-2 AGN lying above the dividing line shown as the dashed green line and all the collected 44501 H II galaxies lying below the dividing line shown as the solid green line. The solid purple line shows the dividing line between Seyfert-2 galaxies and LINERs in this manuscript. The color bar in the top corner represents the corresponding number densities.

Furthermore, besides the database "GalSpecIndx" provided parameter Dn4000 (parameter d4000_n in the database), Dn4000 are re-measured through the downloaded SDSS spectra. The 4000Å break strength $Dn4000 = \frac{\mathrm{Con}_R}{\mathrm{Con}_B}$ can be measured by the definition described in Balogh et al. (1999), Kauffmann et al. (2003b), with Con_B and Con_R as mean continuum emission intensities within the resting wavelength from 3850 to 3950 Å and from 4000 to 4100 Å. Here, we do not show further discussions on our measured Dn4000, but there is quite consistent Dn4000 between our measured values and the reported values in "GalSpecIndx" for the narrow emission line galaxies, with the Spearman Rank correlation coefficient larger than 0.9, to support the reliability of our measured Dn4000.

Based on the measured narrow line emission flux ratios of [O III]λ5007Å to narrow Hβ (O3HB) and [N II]λ6583Å to narrow Hα (N2HA) applied in the BPT diagram, the dividing line in Kewley et al. (2001)

$$\log(\mathrm{O3HB}) = \frac{0.61}{\log(\mathrm{N2HA}) - 0.47} + 1.19 \quad (1)$$

is accepted to collect 14031 Type-2 AGN and to exclude the composite objects in our collected Type-2 AGN. The mean spectrum of the 14031 Type-2 AGN is shown in the left panel of Figure 1. Meanwhile, the dividing line in Kauffmann et al. (2003a)

$$\log(\mathrm{O3HB}) = \frac{0.61}{\log(\mathrm{N2HA}) - 0.05} + 1.30 \quad (2)$$

is accepted to collect 44501 H II galaxies and to exclude the composite objects in our collected H II galaxies. The BPT diagram of O3HB versus N2HA and the applied dividing lines are shown in Figure 2.

Based on the measured Dn4000 and the line parameters of narrow emission lines, it is interesting to check the dependence of the Dn4000 on the narrow emission line properties.

3. Main Results and Discussions

For the collected 14,031 Type-2 AGN, correlations between Dn4000 and log(N2HA) and between Dn4000 and log(O3HB) are shown in the top panels of Figure 3. The Spearman Rank correlation coefficients are about −0.39 ($P_{\mathrm{null}} < 10^{-15}$) and 0.53 ($P_{\mathrm{null}} < 10^{-15}$) for the D$n$4000 versus O3HB and for the Dn4000 versus N2HA, respectively, indicating the Dn4000 more sensitively depends on the N2HA than on the O3HB. For the stronger correlation between Dn4000 and log(N2HA) in Type-2 AGN, after considering the uncertainties in both coordinates, the corresponding best fitting results can be determined by the commonly applied least trimmed squares (LTS) robust technique (Cappellari et al. 2013; Mahdi &

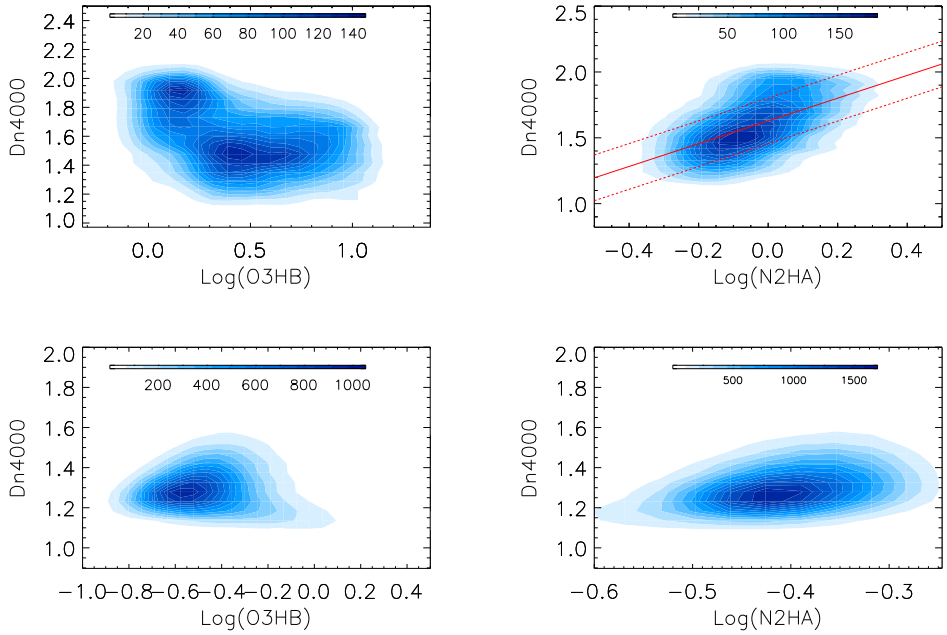

Figure 3. On the correlations between Dn4000 and O3HB (left panels) and between Dn4000 and N2HA (right panels) in the collected Type-2 AGN (top panels) and H II galaxies (bottom panels). In the top right panel, the solid red line and dashed red lines show the best-fitting results and the corresponding 1RMS scatters.

Mohammad 2017)

$$Dn4000 = (1.628 \pm 0.002) + (0.864 \pm 0.011)\log(\mathrm{N2HA}) \quad (3)$$

with the rms scatter about 0.174. Meanwhile, considering larger O3HB leading to stronger central AGN activity, Type-2 AGN with stronger AGN activity (larger O3HB) should have younger stellar ages, which are consistent with the conclusions in Kauffmann et al. (2003a) that the host galaxies of high-luminosity AGN have much younger mean stellar ages.

Moreover, the dependence of Dn4000 on O3HB and on N2HA are also checked in the collected 44501 H II galaxies and shown in the bottom panels of Figure 3. The Spearman Rank correlation coefficients are about 0.01 ($P_{\rm null} < 10^{-15}$) and 0.37 ($P_{\rm null} < 10^{-15}$) for the Dn4000 versus O3HB and for the Dn4000 versus N2HA in the H II galaxies, respectively, indicating weak dependence of Dn4000 on the narrow line flux ratios in H II galaxies. Furthermore, as the results shown in Figure 3, there are similar spans of the applied N2HA in the Type-2 AGN with log(N2HA) $\in$ [~-0.3, ~0.3] and in the H II galaxies with log(N2HA) $\in$ [~-0.55, ~-0.25], therefore, the different dependence of Dn4000 on N2HA between Type-2 AGN and H II galaxies are not due to different spans of the applied N2HA. Actually, the span of log(N2HA) is slightly larger in the Type-2 AGN, if there were effects of the spans, more loose dependence of Dn4000 on N2HA should be expected in the Type-2 AGN.

Besides the dependence of Dn4000 on O3HB and N2HA applied in the known BPT diagrams, dependence of Dn4000 on narrow line luminosities are also checked in Type-2 AGN and in H II galaxies, and shown in Figure 4. The correlations between Dn4000 and [O III]λ5007Å line luminosity ($L_{\rm O3}$) have Spearman rank correlation coefficients about -0.66 ($P_{\rm null} < 10^{-15}$) and -0.53 ($P_{\rm null} < 10^{-15}$) in Type-2 AGN and in H II galaxies, respectively. And the correlations between Dn4000 and narrow Hα line luminosity ($L_{\rm H\alpha}$) have Spearman rank correlation coefficients about -0.70 ($P_{\rm null} < 10^{-15}$) and -0.55 ($P_{\rm null} < 10^{-15}$) in Type-2 AGN and in H II galaxies, respectively. And for the stronger correlations between Dn4000 and $L_{\rm H\alpha}$ and between Dn4000 and $L_{\rm O3}$ in Type-2 AGN, with considering the uncertainties in both coordinates, the corresponding best-fitting results can be determined by the commonly applied LTS robust technique

$$\begin{aligned} Dn4000 &= (11.811 \pm 0.085) \\ &\quad - (0.253 \pm 0.002)\log\left(\frac{L_{\rm H\alpha}}{\rm erg\cdot s^{-1}}\right) \\ Dn4000 &= (9.569 \pm 0.075) \\ &\quad - (0.198 \pm 0.002)\log\left(\frac{L_{\rm O3}}{\rm erg\cdot s^{-1}}\right) \end{aligned} \quad (4)$$

with the rms scatters about 0.143 and 0.155, respectively.

In Type-2 AGN, the dependence of Dn4000 on N2HA and on narrow Hα line luminosity is apparent with linear correlation coefficients of 0.53 and -0.70, but not strong enough. Probably, combining narrow emission line flux ratios and the emission line luminosities could lead to a stronger linear correlation on the Dn4000 parameter. Here, a new

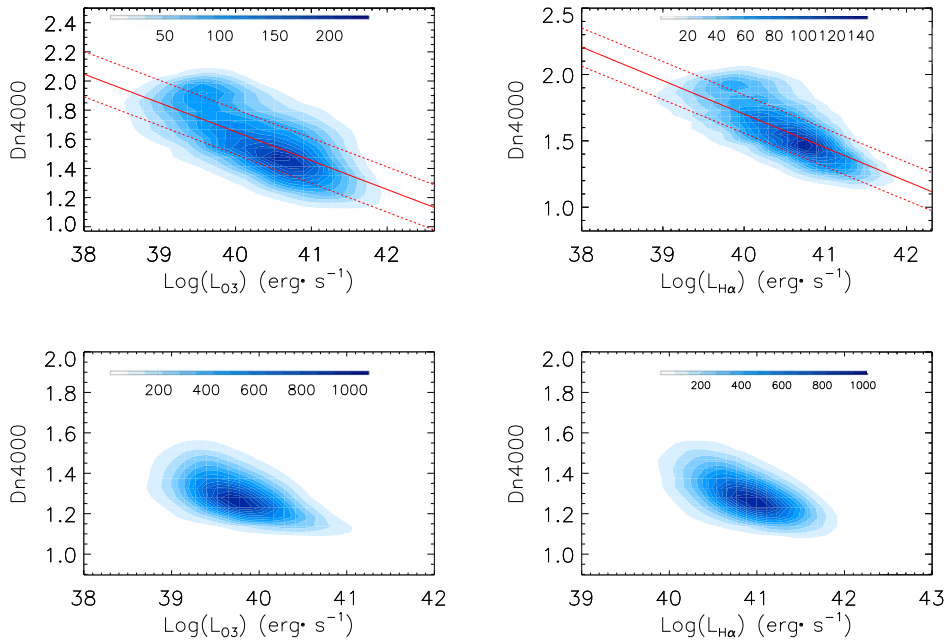

Figure 4. On the correlations between Dn4000 and L_{O3} (left panels) and between Dn4000 and $L_{H\alpha}$ (right panels) in the collected Type-2 AGN (top panels) and in the H II galaxies (bottom panels). In each top panel, the solid red line and dashed red lines show the best fitting results and the corresponding 1RMS scatters.

parameter LR is defined as

$$\mathrm{LR} = 0.2 \times \log(L_{\mathrm{H}\alpha}\ \mathrm{erg}^{-1} \cdot\ \mathrm{s}^{-1}) - 0.5 \times \log(\mathrm{N2HA}) \quad (5)$$

The left panel of Figure 5 shows the correlation between Dn4000 and the new parameter LR in the Type-2 AGN, with the Spearman rank correlation coefficient about -0.76 ($P_{\mathrm{null}} < 10^{-15}$). Meanwhile, the right panel of Figure 5 shows the correlation between the Dn4000 and the new parameter LR in the H II galaxies, with the Spearman rank correlation coefficient about -0.65 ($P_{\mathrm{null}} < 10^{-15}$). The correlations between Dn4000 and the LR in Type-2 AGN and in H II galaxies can be determined by the LTS robust technique

$$\begin{aligned} Dn4000 &= (10.377 \pm 0.056) \\ &\quad - (1.084 \pm 0.007)\mathrm{LR\ (AGN)} \\ Dn4000 &= (7.569 \pm 0.029) \\ &\quad - (0.747 \pm 0.003)\mathrm{LR\ (H\ II)} \end{aligned} \quad (6)$$

with the rms scatters at about 0.125 and 0.069, respectively. Here, simple descriptions are given on the determined formula of the LR. Accepted the formula $\mathrm{LR} = A \times \log(L_{\mathrm{H}\alpha}\ \mathrm{erg}^{-1} \cdot\ \mathrm{s}^{-1}) + B \times \log(\mathrm{N2HA})$ with A and B randomly collected values from -10 to 10, after checking the corresponding Spearman Rank correlation coefficients SR for the correlation between the LR and $Dn4000$, the maximum SR leads to the accepted $A = 0.2$ and $B = -0.5$. Moreover, among all the emission line parameters, the LR of combining Hα luminosity ($0.2\log(L_{\mathrm{H}\alpha})$ and N2HA ($-0.5\log(\mathrm{N2HA})$) leads to the strongest linear correlation between Dn4000 and the LR. And there are no further discussions of the LR combining with different other narrow emission line parameters.

Besides the results shown and discussed above, LINERs (low-ionization nuclear emission line regions) (Heckman 1980; Filippenko & Terlevich 1992; Dopita & Sutherland 1996; Marquez et al. 2017) are included in the sample of Type-2 AGN. LINERs and commonly classified Seyfert-2 galaxies lie in two apparently different sub-branches in the BPT diagrams. Therefore, it is necessary and interesting to check whether LINERs have apparent effects on the results on Dn4000. Here, we do not discuss whether LINERs are genuine AGNs. How to classify LINERs in the BPT diagrams have been well discussed in Groves et al. (2006), Kewley et al. (2006), Juneau et al. (2011), Coldwell et al. (2018), Agostino et al. (2021). There are no further discussions on classifications of LINERs in BPT diagrams. In the BPT diagram of O3HB versus N2HA in Figure 2, considering the dividing lines shown as the dashed green line and solid purple line, there are 4134 classified LINERs lying above the dashed green line and below the solid purple line. Here, there are no further discussions on the dividing line between Seyfert-2 galaxies and LINERs in the BPT diagram of O3HB versus N2HA. However, if the classifications of LINERs are accepted through the dividing lines reported in the BPT diagram of O3HB versus S2HA (flux ratio of [S II] to narrow Hα) reported in Kewley et al. (2006), the corresponding locations of LINERs and Seyfert-2 galaxies in the BPT diagram of O3HB versus N2HA can roughly lead to the dividing line shown as the purple solid line in Figure 2.

Figure 6 shows the corresponding dependence of Dn4000 in the 9897 Seyfert-2 galaxies and in the 4134 LINERs. The correlations between Dn4000 and N2HA have Spearman rank

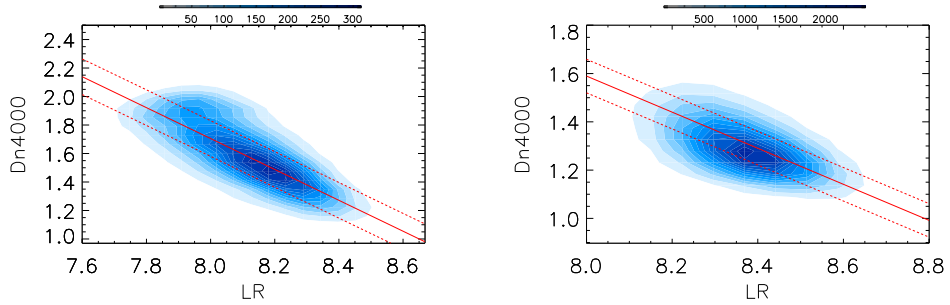

Figure 5. On the correlations between Dn4000 and LR $= 0.2\log(L_{\rm H\alpha}) - 0.5\log({\rm N2HA})$ in the Type-2 AGN (left panel) and in H II galaxies (right panel). The solid red line and dotted red lines show the best-fitting results to the correlation and the corresponding 1RMS scatters, respectively.

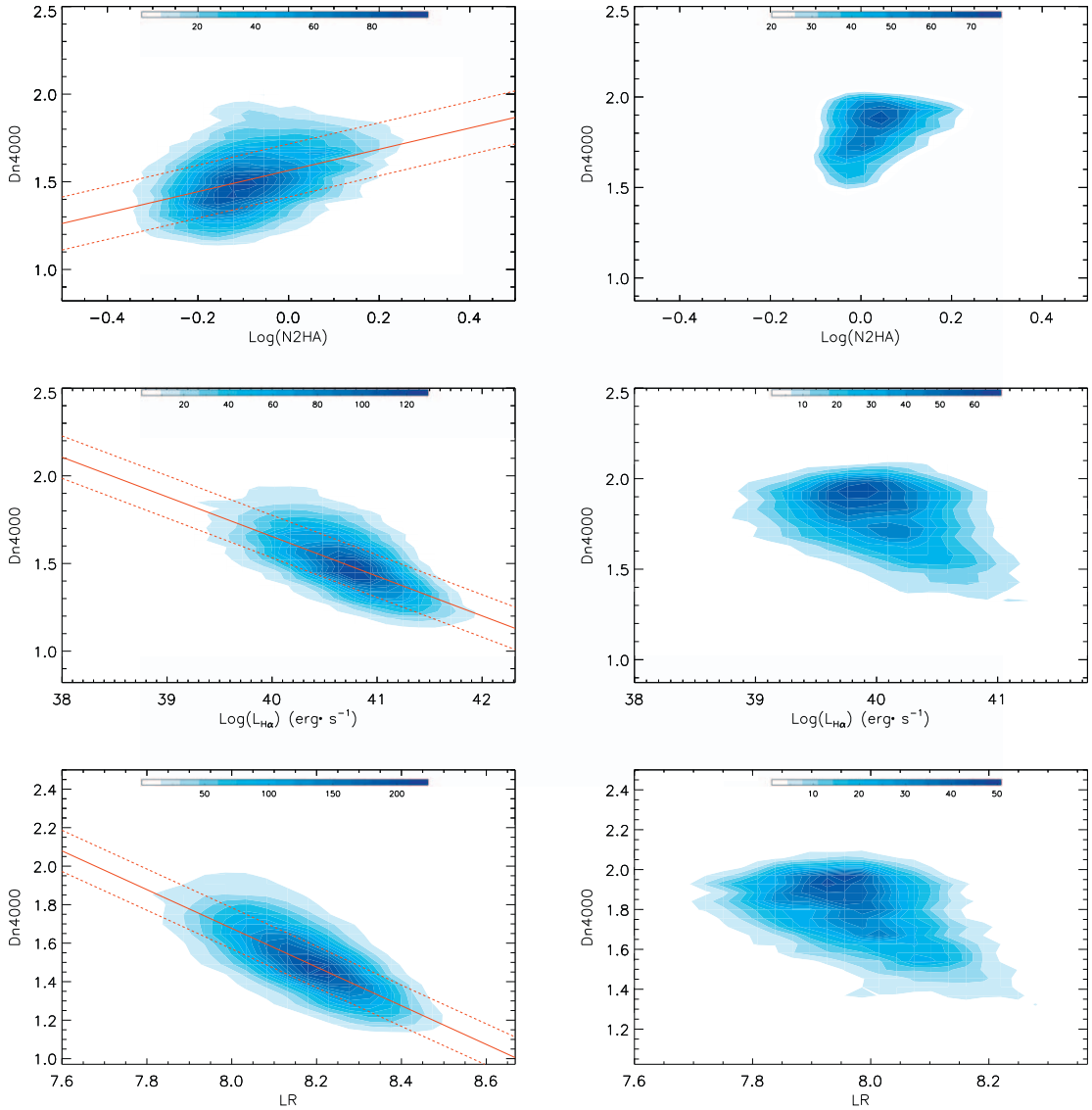

Figure 6. On the correlations between Dn4000 and N2HA (top panels) and between Dn4000 and $L_{\rm H\alpha}$ (middle panels) and between Dn4000 and LR (bottom panels) in the Seyfert-2 galaxies (left panels) and in LINERs (right panels). In each left panel, the solid red line, and dotted red lines show the best-fitting results to the correlation and the corresponding 1RMS scatters, respectively.

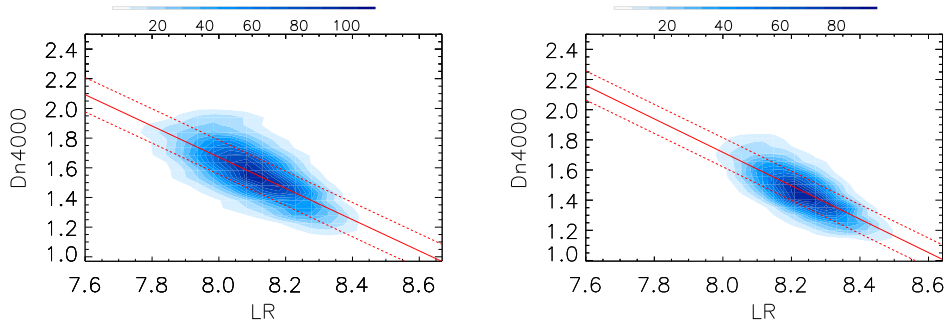

Figure 7. On the correlation between Dn4000 and LR in the Seyfert-2 galaxies with redshift smaller than 0.1 (left panel) and with redshift larger than 0.1 (right panel). In each panel, the solid red line and dotted red lines show the best fitting results to the correlation and the corresponding 1RMS scatters, respectively.

correlation coefficients about 0.40 ($P_{\rm null} < 10^{-15}$) and 0.25 ($P_{\rm null} < 10^{-15}$) in the Seyfert-2 galaxies and in the LINERs, respectively. The correlations between Dn4000 and $L_{\rm H\alpha}$ have Spearman rank correlation coefficients about -0.66 ($P_{\rm null} < 10^{-15}$) and -0.37 ($P_{\rm null} < 10^{-15}$) in the Seyfert-2 galaxies and in the LINERs, respectively. The correlations between Dn4000 and LR have Spearman rank correlation coefficients about -0.72 ($P_{\rm null} < 10^{-15}$) and -0.42 ($P_{\rm null} < 10^{-15}$) in the Seyfert-2 galaxies and in the LINERs, respectively. The very different correlations probably indicate LINERs having unique physical properties different from Seyfert-2 galaxies. Meanwhile, the linear correlations in the 9897 Seyfert-2 galaxies can be determined by the LTS technique

$$\begin{aligned} Dn4000 &= (1.565 \pm 0.002) \\ &\quad + (0.605 \pm 0.012)\log(\mathrm{N2HA}) \\ Dn4000 &= (10.706 \pm 0.094) \\ &\quad - (0.226 \pm 0.002)\log\left(\frac{L_{\rm H\alpha}}{\mathrm{erg \cdot s^{-1}}}\right) \\ Dn4000 &= (9.717 \pm 0.067) - (1.005 \pm 0.008)\mathrm{LR} \end{aligned} \quad (7)$$

with the rms scatters about 0.151, 0.121 and 0.107, respectively. It is clear that LINERs have few effects on the shown results on Dn4000 traced by emission line parameters in Type-2 AGN. Meanwhile, the dependence of Dn4000 on emission line properties are much weaker in LINERs than in normal Seyfert-2 galaxies.

Before ending the section, seven additional points should be noted as follows.

For the first point, it should be necessary to discuss the effects of spectral signal-to-noise (S/N) on the final results, because only the low redshift narrow emission line Type-2 AGN with S/N > 10 are considered, as discussed in Section 2. Among the collected 9897 Seyfert-2 galaxies (LINERs not considered), correlations between Dn4000 and N2HA and between Dn4000 and $L_{\rm H\alpha}$ and between Dn4000 and LR are carefully checked for the 3503 Seyfert-2 galaxies with S/N > 20. The correlations have corresponding Spearman rank correlation coefficients about 0.34 ($P_{\rm null} < 10^{-15}$), about -0.67 ($P_{\rm null} < 10^{-15}$) and about -0.71 ($P_{\rm null} < 10^{-15}$) for the Seyfert-2 galaxies with S/N > 20. Here, the correlations are not shown for the 3503 Seyfert-2 galaxies with S/N > 20, but are well consistent with the results for all the 9897 Seyfert-2 galaxies. Therefore, there are few effects of spectral S/N on our final results.

For the second point, the effects of different redshift on the dependence of Dn4000 on the LR in Type-2 AGN is checked. Among the 9897 Seyfert-2 galaxies (LINERs not considered), correlations between Dn4000 and LR are carefully checked for the 4581 Seyfert-2 galaxies with $z > 0.1$ (Spearman rank correlation coefficient about -0.68 with $P_{\rm null} < 10^{-15}$) and the 5316 Seyfert-2 galaxies with $z < 0.1$ (Spearman rank correlation coefficient about -0.69 with $P_{\rm null} < 10^{-15}$). Here, the critical value $z \sim 0.1$ is applied only because there are similar numbers of objects with $z < 0.1$ and with $z > 0.1$. The correlations are shown in Figure 7 with the LTS technique determined linear correlations described by

$$\begin{aligned} Dn4000 &= (10.088 \pm 0.104) \\ &\quad - (1.052 \pm 0.013)\mathrm{LR}\ (z < 0.1) \\ Dn4000 &= (10.582 \pm 0.116) \\ &\quad - (1.108 \pm 0.014)\mathrm{LR}\ (z > 0.1) \end{aligned} \quad (8)$$

with the rms scatters about 0.116 and 0.096, respectively, well consistent with the results for all the 9897 Seyfert-2 galaxies. Therefore, for Type-2 AGN with redshift less than 0.35, there are no evolution effects on the correlation between Dn4000 and LR.

For the third point, dependence of the correlation between Dn4000 and LR in Type-2 AGN on central activity traced by O3HB is checked. Among the 9897 Seyfert-2 galaxies (LINERs not considered), correlations between Dn4000 and LR are carefully checked for the 4925 Seyfert-2 galaxies with $\log(\mathrm{O3HB}) < 0.56$ (Spearman rank correlation coefficient about -0.77 with $P_{\rm null} < 10^{-15}$) and the 4972 Seyfert-2 galaxies with $\log(\mathrm{O3HB}) > 0.56$ (Spearman rank correlation coefficient of about -0.68 with $P_{\rm null} < 10^{-15}$). Here, the critical value $\log(\mathrm{O3HB}) \sim 0.56$ is applied only because there are similar numbers of objects with $\log(\mathrm{O3HB}) < 0.56$ and

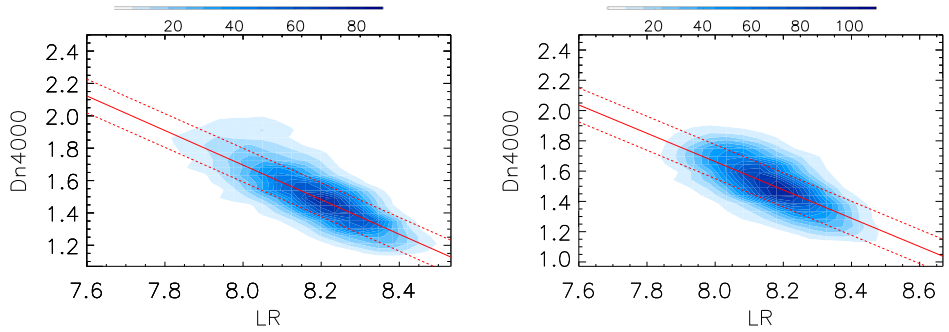

Figure 8. On the correlation between Dn4000 and LR in the Seyfert-2 galaxies with log(O3HB) < 0.56 (left panel) and with log(O3HB) > 0.56 (right panel). In each panel, the solid red line and dotted red lines show the best-fitting results to the correlation and the corresponding 1RMS scatters, respectively.

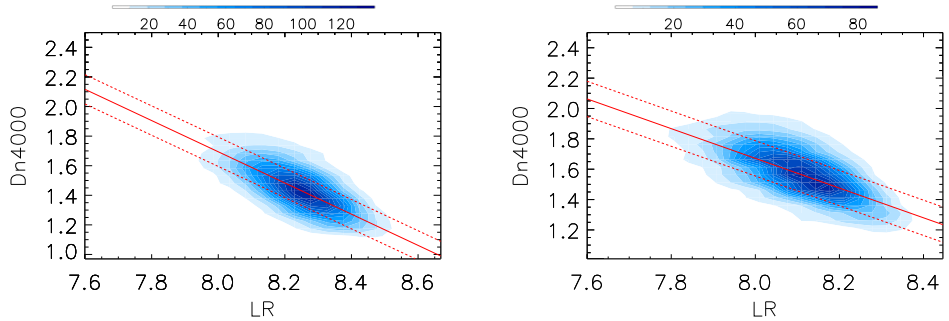

Figure 9. On the correlation between Dn4000 and LR in the Seyfert-2 galaxies with log(N2HA) < -0.091 (left panel) and with log(N2HA) > -0.091 (right panel). In each panel, the solid red line and dotted red lines show the best-fitting results to the correlation and the corresponding 1RMS scatters, respectively.

with log(O3HB) > 0.56. The correlations are shown in Figure 8 with the LTS technique determining linear correlations described by

$$\begin{aligned} Dn4000 &= (10.239 \pm 0.093) - (1.068 \pm 0.012) \\ &\quad \times \mathrm{LR}\ (\log(\mathrm{O3HB}) < 0.56) \\ Dn4000 &= (9.148 \pm 0.099) - (0.936 \pm 0.013) \\ &\quad \times \mathrm{LR}\ (\log(\mathrm{O3HB}) > 0.56) \end{aligned} \tag{9}$$

with the rms scatters about 0.104 and 0.112, respectively, well consistent with the results for all the 9897 Seyfert-2 galaxies. Therefore, for the Type-2 AGN in the BPT diagram, there is no dependence of the correlation between Dn4000 and LR on central activity.

For the fourth point, it is necessary to check probable effects of the applied range of N2HA on the dependence of Dn4000 on LR. Among the 9897 Seyfert-2 galaxies (LINERs not considered), correlations between Dn4000 and LR are carefully checked for the 4987 Seyfert-2 galaxies with log(N2HA) < -0.091 (Spearman rank correlation coefficient about -0.72 with $P_{\mathrm{null}} < 10^{-15}$) and the 4910 Seyfert-2 galaxies with log(N2HA) > -0.091 (Spearman rank correlation coefficient about -0.62 with $P_{\mathrm{null}} < 10^{-15}$). Here, the critical value log(N2HA) ~ -0.091 is applied only because there are similar numbers of objects with log(N2HA) < -0.091 and with log(N2HA) > -0.091. The correlations are shown in Figure 9 with the LTS technique determined linear correlations described by

$$\begin{aligned} Dn4000 &= (10.133 \pm 0.099) \\ &\quad - (1.055 \pm 0.012)\mathrm{LR}\ (\log(\mathrm{N2HA}) < -0.091) \\ Dn4000 &= (9.502 \pm 0.121) \\ &\quad - (0.979 \pm 0.015)\mathrm{LR}\ (\log(\mathrm{N2HA}) > -0.091) \end{aligned} \tag{10}$$

with the rms scatters about 0.099 and 0.116, respectively, well consistent with the results for all the 9897 Seyfert-2 galaxies. Therefore, for the Type-2 AGN in the BPT diagram, there are not any effects of the applied range of N2HA on the dependence of Dn4000 on LR.

For the fifth point, dependence of the correlation between Dn4000 and LR in Type-2 AGN on host galaxy morphology properties traced by inverse concentration parameter IC $= R_{50}/R_{90}$ is checked, where R_{50} and R_{90} represent the radii containing 50% and 90% of the Petrosian flux in the SDSS r band. Among the 9897 Seyfert-2 galaxies (LINERs not considered), there are 9853 Seyfert-2 galaxies with reliable SDSS pipeline provided parameters of R_{50} and R_{90} (parameter name of "petroR50_r" and "petroR50_r" in the SDSS database of "PHOTOOBJALL"). Among the 9853 Seyfert-2 galaxies, correlations between Dn4000 and LR a re carefully checked for the 4943 Seyfert-2 galaxies with IC < 0.374 (Spearman rank correlation coefficient about -0.71 with $P_{\mathrm{null}} < 10^{-15}$) and the 4910 Seyfert-2 galaxies with

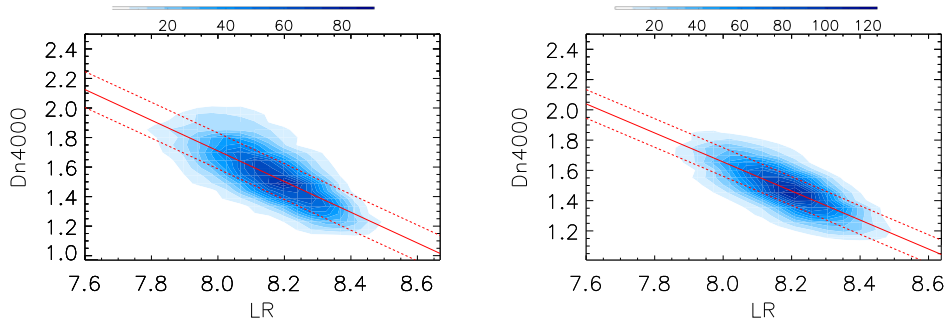

Figure 10. On the correlation between Dn4000 and LR in the Seyfert-2 galaxies with IC < 0.374 (left panel) and with IC > 0.374 (right panel). In each panel, the solid red line and dotted red lines show the best-fitting results to the correlation and the corresponding 1RMS scatters, respectively.

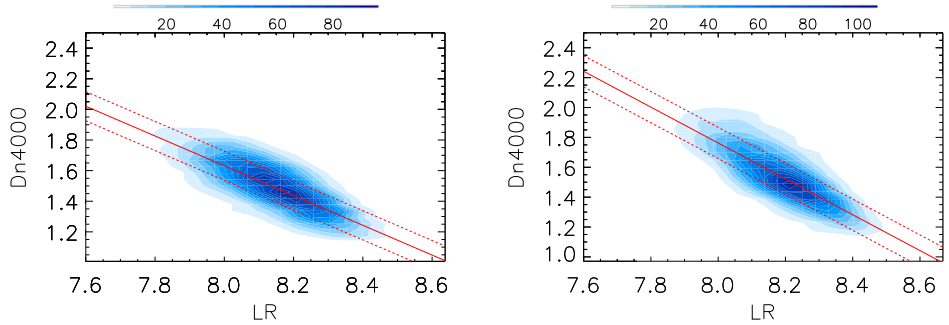

Figure 11. On the correlation between Dn4000 and LR in the Seyfert-2 galaxies with $\sigma_\star < 135$ km s^{-1} (left panel) and with $\sigma_\star > 135$ km s^{-1} (right panel). In each panel, the solid red line and dotted red lines show the best fitting results to the correlation and the corresponding 1RMS scatters, respectively.

IC > 0.374 (Spearman rank correlation coefficient about -0.73 $P_{\rm null} < 10^{-15}$). Here, the critical value IC ~ 0.374 is applied only because there are similar numbers of objects with IC < 0.374 and with IC > 0.374. The correlations are shown in Figure 10 with the LTS technique determined linear correlations described by

$$\begin{aligned} Dn4000 &= (10.022 \pm 0.105) \\ &\quad - (1.039 \pm 0.013){\rm LR}\ ({\rm IC} < 0.374) \\ Dn4000 &= (9.326 \pm 0.089) \\ &\quad - (0.959 \pm 0.011){\rm LR}\ ({\rm IC} > 0.374) \end{aligned} \quad (11)$$

with the rms scatters about 0.122 and 0.095, respectively, quite consistent with the results for all the 9897 Seyfert-2 galaxies. Therefore, for the Type-2 AGN, there are no dependence of the correlation between Dn4000 and LR on host galaxy morphology properties.

For the sixth point, dependence of the correlation between Dn4000 and LR in Type-2 AGN on stellar velocity dispersion $\sigma_\star$ is checked. Considering the tight connection between stellar velocity dispersion and central BH mass (the known M–σ relation) (Ferrarese & Merritt 2000; Gebhardt et al. 2000; Kormendy & Ho 2013; McConnell & Ma 2013) and the tight connection between total stellar mass and central BH mass (Marconi & Hunt 2003; Haring & Rix 2004; Kormendy & Ho 2013; McConnell & Ma 2013; Suh et al. 2020), the dependence on stellar velocity dispersion will provide clues on the effects of the BH mass and total stellar mass on the correlation between Dn4000 and LR in Type-2 AGN. Among the 9897 Seyfert-2 galaxies (LINERs not considered), correlations between Dn4000 and LR are carefully checked for the 4877 Seyfert-2 galaxies with $\sigma_\star < 135$ km s^{-1} (Spearman rank correlation coefficient about -0.76 with $P_{\rm null} < 10^{-15}$) and the 5020 Seyfert-2 galaxies with $\sigma_\star > 135$ km s^{-1} (Spearman rank correlation coefficient about -0.77 with $P_{\rm null} < 10^{-15}$). Here, the critical value $\sigma_\star \sim 135$ km s^{-1} is applied only because there are similar numbers of objects with $\sigma_\star < 135$ km s^{-1} and with $\sigma_\star > 135$ km s^{-1}. The correlations are shown in Figure 11 with the LTS technique determined linear correlations

$$\begin{aligned} Dn4000 &= (9.408 \pm 0.084) \\ &\quad - (1.006 \pm 0.011){\rm LR}\ (\sigma_\star < 135\ {\rm km\ s^{-1}}) \\ Dn4000 &= (11.365 \pm 0.096) \\ &\quad - (1.201 \pm 0.012){\rm LR}\ (\sigma_\star > 135\ {\rm km\ s^{-1}}) \end{aligned} \quad (12)$$

with the rms scatters at about 0.095 and 0.105, respectively, consistent with the results for all the 9897 Seyfert-2 galaxies. Therefore, for the Type-2 AGN, there are no dependences of the correlation between Dn4000 and LR on host galaxy stellar velocity dispersions.

For the seventh point, motivated by the reported dependence of the Dn4000 on the total stellar mass in Kauffmann et al. (2003a), Zahid & Geller (2017), it is interesting to check which

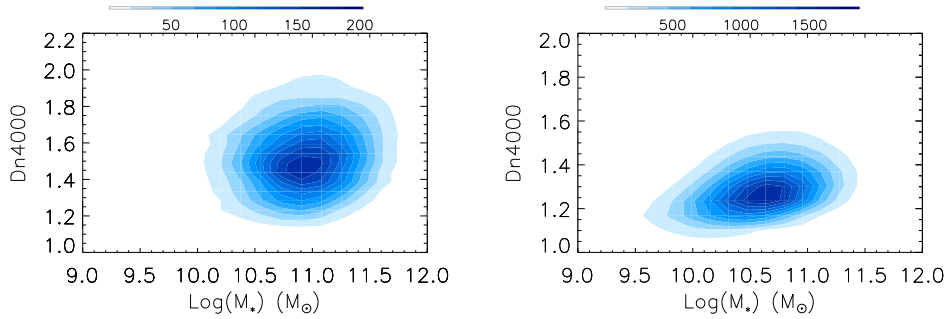

Figure 12. On the correlation between Dn4000 and total stellar mass $M_\star$ in the Seyfert-2 galaxies (left panel) and in the H II galaxies (right panel).

parameter, the parameter LR or the total stellar mass $M_\star$, is preferred to trace the Dn4000. Here, the public database "StellarMassPCAWiscBC03" (Chen et al. 2012) from MPA/JHU research group is accepted to collect the measured total stellar masses of narrow emission line galaxies in SDSS. Then, Figure 12 shows dependence of Dn4000 on the total stellar mass of the collected 9897 Seyfert-2 galaxies (LINERs not considered) and of the collected 44501 H II galaxies, with Spearman rank correlation coefficients about 0.15 ($P_{\rm null} < 10^{-15}$) and 0.39 ($P_{\rm null} < 10^{-15}$) respectively. The results are simply consistent with the results in Kauffmann et al. (2003a) that strong AGN (here, Seyfert-2 galaxies) have weak dependence of the Dn4000 on the $M_\star$. Due to the weakness of the dependence in Figure 12, there are no descriptions on the dependence by formula. The different dependence of Dn4000 on $M_\star$ in Seyfert-2 galaxies and in H II galaxies could be due to AGN feedback leading the host galaxy evolution of AGN to be different from the normal evolution of quiescent galaxies. To discuss the different dependence of Dn4000 on $M_\star$ by the effects of AGN activity is not the objective of this manuscript. However, the results can be applied to support that total stellar mass can be simply applied to trace stellar age (Dn4000) only in quiescent galaxies, whereas the parameter LR can be efficiently applied to trace the stellar age (Dn4000) in both AGN and none-AGN galaxies.

4. Summary and Conclusions

The final summary and conclusions are as follows.

1. Based on well-measured narrow emission lines of low redshift narrow emission line main galaxies in SDSS DR16, large samples of 14,031 Type-2 AGN and 44,501 H II galaxies are collected through applications of the BPT diagram of O3HB versus N2HA.
2. Strong positive correlation between Dn4000 and N2HA and negative correlation between Dn4000 and O3HB can be confirmed in the Type-2 AGN. However, weaker corresponding correlations between Dn4000 and narrow emission line ratios are detected in H II galaxies.
3. Strong negative correlations can be confirmed between Dn4000 and narrow emission line luminosities in both Type-2 AGN and H II galaxies.
4. Combining N2HA and narrow Hα line luminosity, the stronger negative correlation between Dn4000 and LR $= 0.2\log(L_{\rm H\alpha}\ {\rm erg}^{-1}\cdot{\rm s}^{-1}) - 0.5\log({\rm N2HA})$ can be confirmed in Type-2 AGN and in H II galaxies, with smaller rms scatters.
5. Through applications of BPT diagrams, LINERs have weaker dependence of Dn4000 on narrow emission line ratios and narrow line luminosities, indicating different intrinsic physical properties of LINERs from Seyfert-2 galaxies.
6. There are consistent correlations between Dn4000 and *LR* for the Type-2 AGN with different spectral S/N, different redshifts, different O3HB, different N2HA, different host galaxy morphology properties and different host galaxy stellar velocity dispersions, leading to the robust and strong dependence of Dn4000 on the parameter of the LR in Type-2 AGN.
7. Applications of narrow emission line properties to trace the parameter Dn4000 in Type-2 AGN will provide a convenient method to estimate statistical properties of stellar ages of samples of more luminous AGN with weak host galaxy absorption features but with apparent narrow emission lines.

Acknowledgments

Zhang gratefully acknowledge the anonymous referee for giving us constructive comments and suggestions to greatly improve the paper. Zhang gratefully thanks GuangXi University for kind financial support, and NSFC-12173020 and NSFC-12373014 and the the Guangxi Talent Programme (Highland of Innovation Talents) for kind grant support. This manuscript has made use of the data from the SDSS projects. The SDSS-III website is http://www.sdss3.org/. SDSS-III is managed by the Astrophysical Research Consortium for the Participating Institutions of the SDSS-III Collaborations.

References

Agostino, C. J., Salim, S., Faber, S. M., et al. 2021, ApJ, 922, 156
Ahumada, R., Allende Prieto, C., Almeida, A., et al. 2020, ApJS, 249, 3
Balogh, M. L., Morris, S. L., Yee, H. K. C., Carlberg, R. G., & Ellingson, E. 1999, ApJ, 527, 54
Baldwin, J. A., Phillips, M. M., & Terlevich, R. 1981, PASP, 93, 5
Brinchmann, J., Charlot, S., White, S. D. M., et al. 2004, MNRAS, 351, 1151
Bruzual, A. G., & Charlot, S. 1993, ApJ, 405, 538
Cid Fernandes, R., Mateus, A., Sodre, L., Stasinska, G., & Gomes, J. M. 2005, MNRAS, 358, 363
Cappellari, M. 2017, MNRAS, 466, 798
Cappellari, M., Scott, N., Alatalo, K., et al. 2013, MNRAS, 432, 1709
Chen, Y. M., Kauffmann, G., Tremonti, C. A., et al. 2012, MNRAS, 421, 314
Coldwell, G. V., Alonso, S., Duplancic, F., & Valeria, M. 2018, MNRAS, 476, 2457
Comerford, J. M., Negus, J., Muller-Sanchez, F., et al. 2020, ApJ, 901, 159
Dopita, M. A., & Sutherland, R. S. 1996, ApJS, 102, 161
Fabian, A. C. 2012, ARA&A, 50, 455
Ferrarese, F., & Merritt, D. 2000, ApJL, 539, L9
Feruglio, C., Maiolino, R., Piconcelli, E., et al. 2010, A&A, 518, 155
Filippenko, A. V., & Terlevich, R. 1992, ApJL, 397, L79
Gebhardt, K., Bender, R., Bower, G., et al. 2000, ApJL, 539, L13
Greene, J. E., Setton, D., Bezanson, R., et al. 2020, ApJL, 899, L9
Groves, B., Kewley, L., Kauffmann, G., & Heckman, T. 2006, NewAR, 50, 743
Haring, N., & Rix, H. W. 2004, ApJL, 604, L89
Heckman, T. M. 1980, A&A, 87, 152
Heckman, T. M., & Best, P. N. 2014, ARA&A, 52, 589
Juneau, S., Dickinson, M., Alexander, D. M., & Salim, S. 2011, ApJ, 736, 104
Kewley, L. J., Dopita, M. A., Sutherland, R. S., Heisler, C. A., & Trevena, J. 2001, ApJ, 556, 121
Kewley, L. J., Groves, B., Kauffmann, G., & Heckman, T. 2006, MNRAS, 372, 961
Kewley, L. J., Nicholls, D. C., & Sutherland, R. S. 2019, ARA&A, 57, 511
Kauffmann, G., Heckman, T. M., Tremonti, C., et al. 2003a, MNRAS, 346, 1055
Kauffmann, G., Heckman, T. M., White, S. D. M., et al. 2003b, MNRAS, 341, 33
King, A., & Pounds, K. 2015, ARA&A, 53, 115
Kormendy, J., & Ho, L. C. 2013, ARA&A, 51, 511
Mahdi, R., & Mohammad, A. 2017, J. Stat. Comp. Sim., 87, 1130
Marconi, A., & Hunt, L. K. 2003, ApJL, 589, L21
McConnell, N. J., & Ma, C. P. 2013, ApJ, 764, 184
Marquez, I., Masegosa, J., Gonzalez-Martin, O., et al. 2017, FrASS, 4, 34
McNamara, B. R., & Nulsen, P. E. J. 2007, ARA&A, 45, 117
Muller-Sanchez, F., Nevin, R., Comerford, J. M., et al. 2018, Natur, 556, 315
Netzer, H. 2015, ARA&A, 53, 365
Page, M. J., Symeonidis, M., Vieira, J. D., et al. 2012, Natur, 485, 213
Shin, J., Woo, J. H., Chung, A., et al. 2019, ApJ, 881, 147
Suh, H., Civano, F., Hasinger, G., et al. 2019, ApJ, 872, 168
Suh, H., Civano, F., Trakhtenbrot, B., et al. 2020, ApJ, 889, 32
Tombesi, F., Melendez, M., Veilleux, S., et al. 2015, Natur, 519, 436
Tremonti, C. A., Heckman, T. M., Kauffmann, G., et al. 2004, ApJ, 613, 898
Wylezalek, D., & Zakamska, N. L. 2016, MNRAS, 461, 3724
Zahid, H. J., Damjanov, I., Geller, M. J., & Chilingarian, I. 2015, ApJ, 806, 122
Zahid, H. J., & Geller, M. J. 2017, ApJ, 841, 32
Zhang, X. G. 2021a, ApJ, 909, 16
Zhang, X. G. 2021b, ApJ, 919, 13
Zhang, X. G. 2021c, MNRAS, 507, 5205
Zhang, X. G. 2022a, ApJS, 261, 23
Zhang, X. G. 2022b, ApJS, 260, 31
Zhang, X. G. 2023, ApJS, 267, 36
Zhang, X. G. 2024a, ApJ, 964, 141
Zhang, X. G., Feng, Y. Q., Chen, H., & Yuan, Q. R. 2020, ApJ, 905, 97
Zinn, P. C., Middelberg, E., Norris, R. P., et al. 2013, ApJ, 774, 66
Zubovas, K., Nayakshin, S., King, A., et al. 2013, MNRAS, 433, 3079